

Deep inelastic diffractive scattering at HERA

Pierre Van Mechelen^{a*},

^aUniversiteit Antwerpen, Pierre.VanMechelen@ua.ac.be

Recent high precision measurements of deep inelastic diffractive scattering at HERA are presented in an increased region of phase space. Current models for diffractive photon dissociation are compared to the data.

1. Introduction

It is well known that soft hadron-hadron scattering can be described by Regge phenomenology, which models the total, elastic and single and double diffractive dissociation cross sections in terms of reggeon and pomeron exchange [1]. At high energies, it is the pomeron exchange mechanism that dominates the total cross section [2]. However, until recently, our understanding of the pomeron in terms of Quantum Chromodynamics (QCD) [3] remained fragmentary, at best.

The observation of events with a large rapidity gap in the hadronic final state at HERA [4], which are attributed to diffractive dissociation of (virtual) photons, led to a renewed interest in the study of the underlying dynamics of diffraction. In deep inelastic ep scattering, the long hadronic lifetime of the photon at small Bjorken- x allows to make the link with diffractive dissociation in hadron-hadron scattering, while the presence of one or more hard scales, such as the (variable) virtuality Q^2 , enables perturbative calculations in QCD.

In the framework of QCD, it is tempting to attribute a partonic structure to the pomeron [5]; an approach which proves to be very successful in describing various aspects of diffractive virtual photon dissociation. QCD calculations indicate, however, that the pomeron does not exhibit a universal behaviour over the full kinematic range. Indeed, experimentally a transition is observed when going from the soft to the hard scattering

regime; the effective intercept of the pomeron trajectory changes from 1.08 in the soft limit to 1.2 in harder interactions.

Early experimental measurements at HERA of the inclusive cross section [6] led to the conclusion that a partonic pomeron would be dominated by hard gluons. This has been confirmed by investigations of the hadronic final state of diffractive photon dissociation ranging from the study of inclusive particle spectra to exclusive hard jet and open charm production [7].

This article presents recent high precision measurements of the inclusive diffractive deep inelastic cross section in an increased region of phase space. Section 2 presents the experimental data together with a new NLO QCD fit of the diffractive parton densities. Current models for diffractive photon dissociation are subsequently compared to the data in Sec. 3. A summary is given in Sec. 4.

2. Experimental data

2.1. Cross section measurements

In addition to the usual DIS kinematic variables, the photon virtuality Q^2 and the Bjorken scaling variables x and y , in the case of diffractive DIS one introduces the variables $x_{\mathcal{P}}$ and β , defined respectively as the longitudinal momentum fraction of the proton carried by the colourless exchange causing the rapidity gap, and the longitudinal momentum fraction of the colourless exchange carried by the struck quark. The variable

*Postdoctoral fellow of the Fund for Scientific Research - Flanders (Belgium)

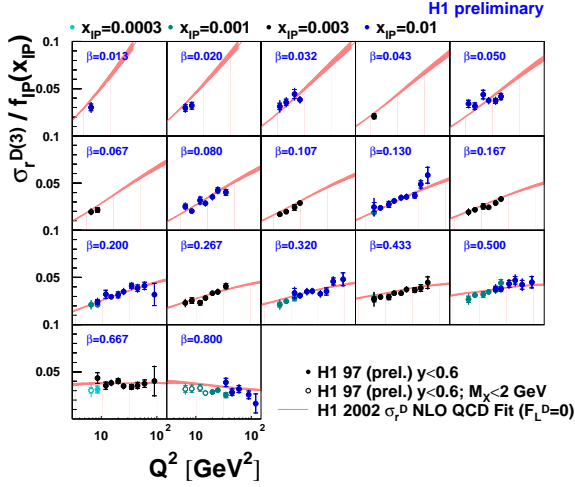


Figure 1. The diffractive reduced cross section divided by the pomeron flux as a function of Q^2 in bins of β and for different $x_{\mathbb{P}}$ values. The band represents the result of the NLO QCD fit discussed in Sec. 2.2.

β in the γP^2 collision is analogous to Bjorken- x in γp interactions.

Figure 1 shows recent measurements obtained by the H1 Collaboration. The preliminary results are presented as a reduced cross section, $\sigma_r^{D(3)}$, defined through

$$\frac{d^3\sigma^D}{dx_{\mathbb{P}}dx dQ^2} = \frac{4\pi\alpha^2}{xQ^4} \left(1 - y + \frac{y^2}{2}\right) \times \sigma_r^{D(3)}(x_{\mathbb{P}}, x, Q^2) \quad (1)$$

and divided by the ‘‘pomeron flux’’ $f_{\mathbb{P}}(x_{\mathbb{P}})$. This reduced cross section is equal to the conventional diffractive structure function, $F_2^{D(3)}$, up to corrections due the longitudinal structure function, $F_L^{D(3)}$. The pomeron flux factor is obtained from a parametrization of the $x_{\mathbb{P}}$ dependence of the cross section inspired by Regge theory. The parametrization works well, as can be seen from

² \mathbb{P} is a generic label for the colourless exchange, which in some models is identified as the pomeron.

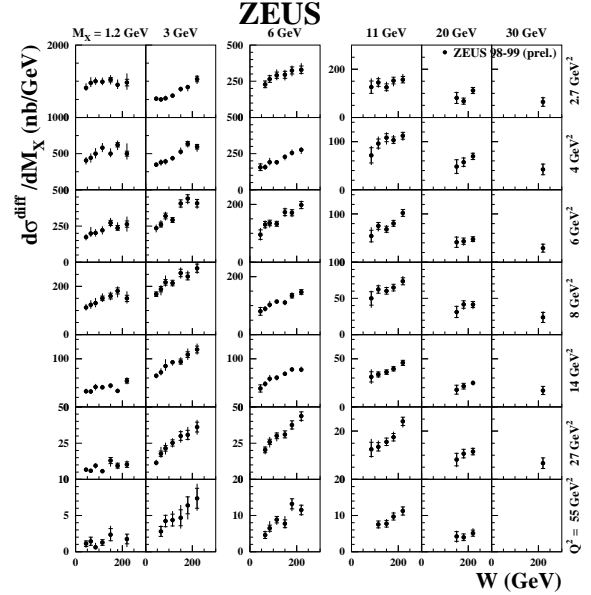


Figure 2. The diffractive differential cross section, $d\sigma/dM_X$, as a function of W in bins of M_X and Q^2 .

the overlap of data points at the same β and Q^2 values obtained for different proton momentum losses $x_{\mathbb{P}}$. The intercept of the pomeron trajectory extracted from this data is

$$\alpha_{\mathbb{P}} = 1.173 \pm 0.018 \text{ (stat.)} \pm 0.017 \text{ (syst.)}_{-0.035}^{+0.063} \text{ (model)}. \quad (2)$$

Positive scaling violations are observed in most of the phase space, suggesting a large gluon content of the diffractive exchange. The ratio of the diffractive to inclusive DIS cross sections is found to be reasonably flat at fixed x as a function of Q^2 , indicating that the same scaling violations occur in both processes.

The ZEUS Collaboration has recently installed a new ‘‘Forward Plug’’ calorimeter which covers the range in pseudorapidity $4 < \eta < 5$ and increases the measurable range in mass of the proton dissociation system, M_Y , to 2.3 GeV and hence reduces the background due to proton dissociation. Preliminary results are shown in Fig. 2.

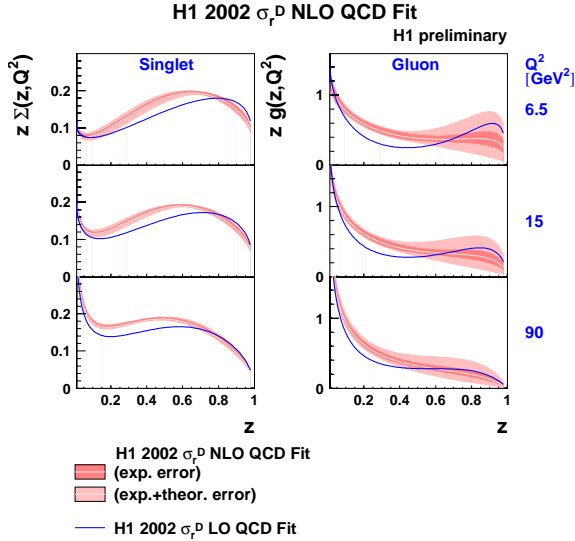


Figure 3. Diffractive quark singlet ($6 * u$ with $u = d = s = \bar{u} = \bar{d} = \bar{s}$) and gluon density. The pomeron flux is normalized to unity at $x_P = 0.003$.

It can be observed that in the resonance production region (where the mass of the photon dissociation system, M_X , is smaller than 2 GeV) there is little dependence on the hadronic mass W , while a strong rise with W is observed at higher M_X for all values of Q^2 . This rise is compatible with the energy dependence of inclusive data.

2.2. Next-to-leading order DGLAP fits

Using a parametrization based on Chebychev polynomials at a starting scale of $Q_0^2 = 3 \text{ GeV}^2$, quark and gluon densities have been fitted to the observed H1 cross section by applying the DGLAP evolution equations. Subleading reggeon exchanges are included assuming the structure function of the pion. The fit, which includes the data shown in Fig. 1 together with data at higher Q^2 shown in Fig. 4, yields $\chi^2/ndf = 308.7/306$.

Figure 3 shows the result of the next-to-leading order (NLO) QCD fit, with full propagation of statistical, systematic experimental and theoretical errors. The momentum fraction carried by

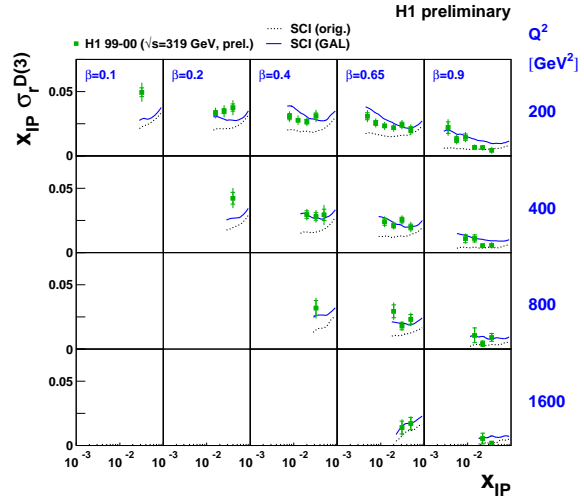


Figure 4. The diffractive reduced cross section, multiplied by x_P , is shown as a function of x_P in bins of β and Q^2 . The curves represent the SCI model with and without the GAL.

gluons is estimated to be $75 \pm 15\%$.

3. Model comparisons

3.1. The Soft Colour Interaction model at large Q^2

A model that does not use the notion of a pomeron at all is the Soft Colour Interaction (SCI) model [8]. Instead, the standard matrix element and parton shower description of deep inelastic scattering is used, which, at low Bjorken- x , is dominated by boson-gluon fusion. In addition, non-perturbative interactions affect the final colour connections between partons, while leaving the parton momenta unchanged. This may result in an interruption of the colour strings between partons, thus creating a large rapidity gap in the final state. The probability for such a SCI has to be fixed by the experimental data.

Figure 4 compares the SCI model to recently obtained data at large Q^2 . While the application of a ‘‘Generalized Area Law’’ (GAL), which favours soft colour interactions that make the colour strings between partons shorter, clearly

improves the description of the data (as is also observed at lower Q^2), systematic deviations occur towards low values of β .

3.2. The Saturation model at low Q^2

In this and the subsequent model, the virtual photon is considered to fluctuate into partonic configurations, e.g. $q\bar{q}$ or $q\bar{q}g$. In the proton rest frame and at low Bjorken- x , this happens long before the actual interaction with the proton. Both states, $q\bar{q}$ and $q\bar{q}g$, can be described by dipole wave-functions [9].

The Saturation model [10] proposes a parametrization for the dipole-proton cross section:

$$\sigma(x, r^2) = \sigma_0 \left[1 - \exp\left(-\frac{r^2}{4R_0^2(x)}\right) \right], \quad (3)$$

with

$$R_0(x) = \frac{1}{\text{GeV}} \left(\frac{x}{x_0}\right)^{\lambda/2}; \quad (4)$$

x_0 and λ are parameters of the model. This parameterization exhibits colour transparency for small dipole sizes, r , and saturation of the cross section towards low x and low Q^2 .

Figure 5 shows that this model consistently lies beneath the measured data points.

3.3. Two-gluon exchange model

This QCD model [11] describes the elastic scattering of $q\bar{q}$ and $q\bar{q}g$ states off the proton through the exchange of two gluons in a net colour-singlet configuration. The perturbative calculation requires large transverse momenta of all outgoing partons and $x_P < 0.01$ to avoid the valence quark region in the proton.

Despite these restrictions, Fig. 6 shows that the model describes the data rather well.

4. Summary

High precision measurements of the diffractive reduced cross section in deep inelastic scattering have been performed by the H1 and ZEUS collaborations in an increased region of phase space. The data support Regge factorization (provided subleading trajectories can contribute) with a value for the pomeron intercept which is larger

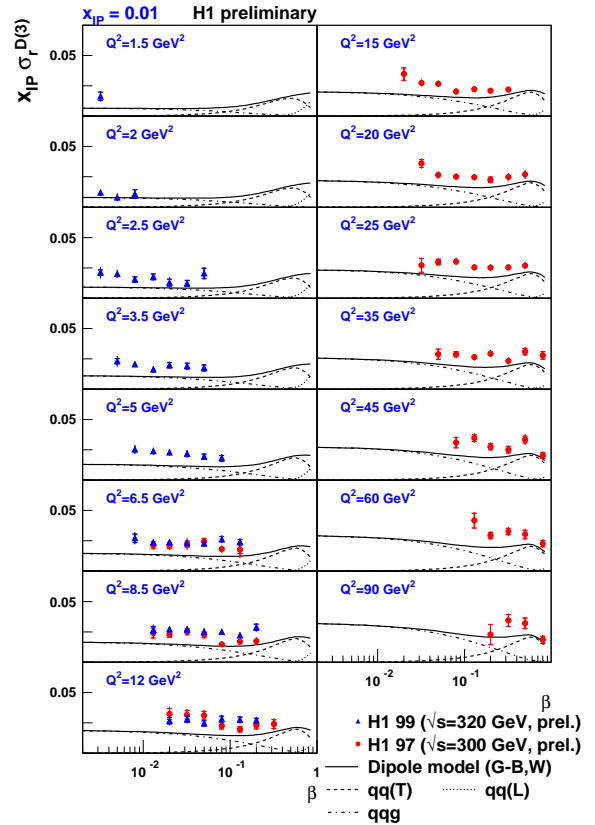


Figure 5. The diffractive reduced cross section, multiplied by x_P , is shown as a function of β at $x_P = 0.01$ and in bins of Q^2 . The curves represent the prediction of the Saturation model decomposed in longitudinal and transverse $q\bar{q}$ and $q\bar{q}g$ contributions.

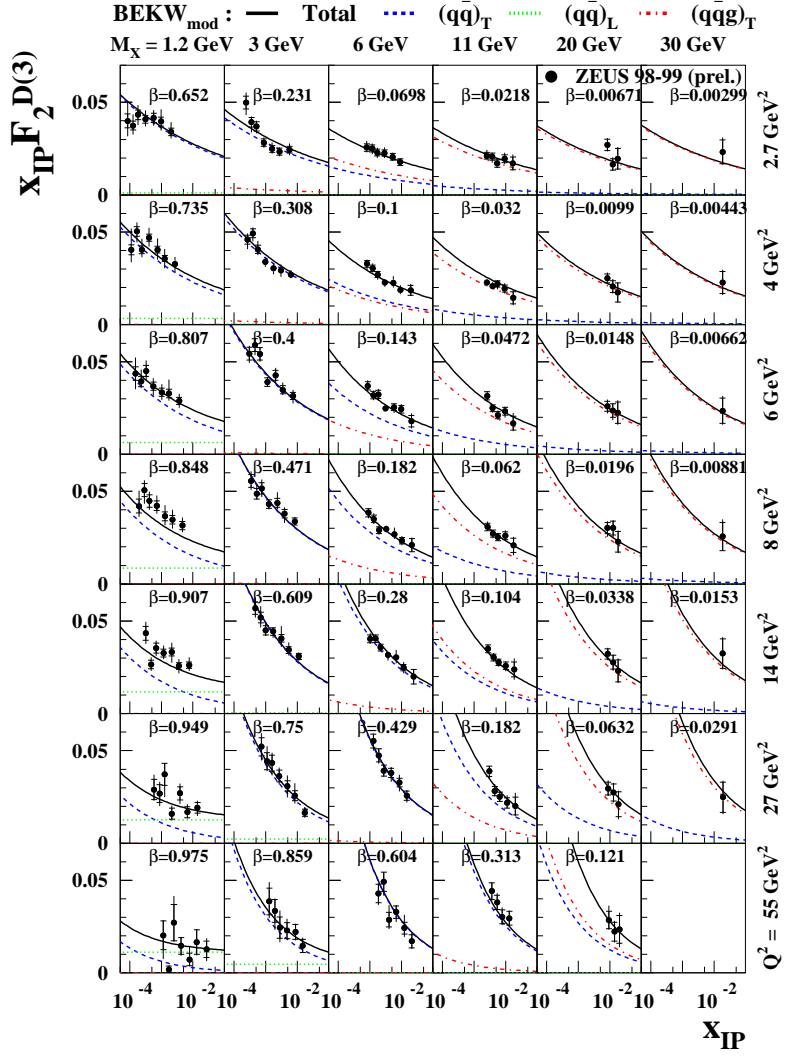


Figure 6. The diffractive structure function, multiplied by $x_{\mathcal{P}}$, is shown as a function of $x_{\mathcal{P}}$ in bins of β and Q^2 . The curves represent the prediction of the 2-gluon exchange model decomposed in longitudinal and transverse $q\bar{q}$ and $q\bar{q}g$ contributions.

than for the soft pomeron. New NLO QCD fits of the diffractive parton densities are available and can be used to test QCD hard scattering factorization. Models describe the data in general, but some new discrepancies are uncovered with the increased accessible phase space.

Acknowledgments

I am indebted to all members of the H1 and ZEUS Collaborations who contributed to these results by collecting and analyzing the experimental data.

REFERENCES

1. P. D. B. Collins, *Introduction to Regge Theory and High Energy Physics*, Cambridge University Press (1977).
2. A. Donnachie and P. V. Landshoff, Phys. Lett. B296 (1992) 227–232.
3. J. R. Forshaw and D. A. Ross, *Quantum Chromodynamics and the Pomeron*, Cambridge University Press (1997).
4. ZEUS Collaboration, M. Derrick et al., Phys. Lett. B315 (1993) 481–493, *ibid.* B346 (1995) 399–414;
H1 Collaboration, T. Ahmed et al., Nucl. Phys. B429 (1994) 477–502, *ibid.* B435 (1995) 3–22.
5. G. Ingelman and P. Schlein, Phys. Lett. B152 (1985) 256.
6. H1 Collaboration, T. Ahmed et al., Phys. Lett. B348 (1995) 681–696, C. Adloff et al., Z. Phys. C76 (1997) 613–629;
ZEUS Collaboration, M. Derrick et al., Z. Phys. C68 (1995) 569–584, *ibid.* C70 (1996) 391–412, J. Breitweg et al., Eur. Phys. J. C1 (1998) 81–96, *ibid.* C6 (1999) 43–66, *ibid.* C25 (2002) 169–187.
7. ZEUS Collaboration, M. Derrick et al., Phys. Lett. B332 (1994) 228–243, *ibid.* B338 (1994) 483–496, Z. Phys. C67 (1995) 227–238, J. Breitweg et al., Phys. Lett. B421 (1998) 368–384, S. Chekanov et al., Phys. Lett. B516 (2001) 273–292, Phys. Rev. D65 (2002) 052001, Phys. Lett. B545 (2002) 244–260;
H1 Collaboration, S. Aid et al., Z. Phys. C70 (1996) 609–620, C. Adloff et al., Phys. Lett. B428 (1998) 206–220, Eur. Phys. J. C1 (1998) 495–507, *ibid.* C5 (1998) 439–452, *ibid.* C6 (1999) 421–436, *ibid.* C20 (2001) 29–49, Phys. Lett. B520 (2001) 191.
8. A. Edin, G. Ingelman and J. Rathsman, Phys. Lett. B366 (1996) 371–378, Z. Phys. C75 (1997) 57–70;
J. Rathsman, Phys. Lett. B452 (1999) 364–371.
9. J. Bartels, J. Ellis, H. Kowalski and M. Wüsthoff, Eur. Phys. J. C7 (1999) 443–458.
10. K. Golec-Biernat, M. Wüsthoff, Phys. Rev. D59 (1999) 014017.
11. J. Bartels, H. Lotter and M. Wüsthoff, Phys. Lett. B379 (1996) 239–248;
J. Bartels, C. Ewerz, H. Lotter and M. Wüsthoff, Phys. Lett. B386 (1996) 389–396;
J. Bartels, H. Jung, M. Wüsthoff, Eur. Phys. J. C11 (1999) 111–125.